ANL/ET/CP- 94714

Estimation of Fatigue Strain-Life Curves for Austenitic Stainless Steels in Light Water Reactor Environments*

Omesh K. Chopra and Jean L. Smith

Energy Technology Division
Argonne National Laboratory
9700 South Cass Avenue
Argonne, Illinois 60439 USA

January 1998

To be presented at the *Symposium on Fatigue & Fracture in Pressure Vessels and Piping*, 1998 ASME/JSME Joint Pressure Vessel and Piping Conference, July 26–30, 1998, Sheraton San Diego Hotel and Marina, San Diego, CA.

*Work supported by the Office of Nuclear Regulatory Research of the U.S. Nuclear Regulatory Commission, under FIN Number W6610; Program Manager: Dr. M. McNeil.

DISCLAIMER

Portions of this document may be illegible in electronic image products. Images are produced from the best available original document.

Estimation of Fatigue Strain-Life Curves for Austenitic Stainless Steels in Light Water Reactor Environments

Omesh K. Chopra and Jean L. Smith

Energy Technology Division
Argonne National Laboratory
Argonne, Illinois 60439

ABSTRACT

The ASME Boiler and Pressure Vessel Code design fatigue curves for structural materials do not explicitly address the effects of reactor coolant environments on fatigue life. Recent test data indicate a significant decrease in fatigue lives of austenitic stainless steels (SSs) in light water reactor (LWR) environments. Unlike those of carbon and low-alloy steels, environmental effects on fatigue lives of SSs are more pronounced in low-dissolved-oxygen (low-DO) water than in high-DO water. This paper summarizes available fatigue strain vs. life data on the effects of various material and loading variables such as steel type, DO level, strain range, and strain rate on the fatigue lives of wrought and cast austenitic SSs. Statistical models for estimating the fatigue lives of these steels in LWR environments have been updated with a larger data base. The significance of the effect of environment on the current Code design curve has been evaluated.

INTRODUCTION

The ASME Boiler and Pressure Vessel Code Section III, Subsection NB,[1] which contains rules for the construction of Class 1 components for nuclear power plants, recognizes fatigue as a possible mode of failure in pressure vessel steels and piping materials. Figures I-9.1 through I-9.6 of Appendix I to Section III of the Code specifies design fatigue curves that define the allowable number of cycles as a function of applied stress amplitude. However, Subsection NB-3121 of Section III of the Code states that the data on which the design fatigue curves are based did not include tests in the presence of corrosive environments that might accelerate fatigue failure. Article B-2131 in Appendix B to Section III states that the owner's design specifications should provide information on any reduction to design curves necessitated by environmental conditions. Recent fatigue strain vs. life (S-N) data[2-11] illustrate potentially significant effects of light water reactor (LWR) coolant environments on the fatigue resistance of carbon and low-alloy steels and austenitic stainless steels (SSs), Fig. 1. Under certain conditions of loading and environment, fatigue lives of carbon steels can be a factor of 70 lower in the environment than those in air. Therefore, the margins in the ASME Code may be less conservative than originally intended.

A program was initiated at Argonne National Laboratory (ANL) to provide data under conditions that are not addressed in the existing data base and to develop models for estimating the fatigue life of primary pressure boundary materials in LWR environments. Based on the existing fatigue S-N data, interim design fatigue curves that address environmental effects on fatigue life of carbon and low-alloy steels and austenitic SSs have been proposed.[12] Statistical models have also been developed at ANL for estimating the effects of various material and loading conditions on fatigue life of these materials.[13,14] Results of the statistical analysis have been used to estimate the probability of fatigue cracking in reactor

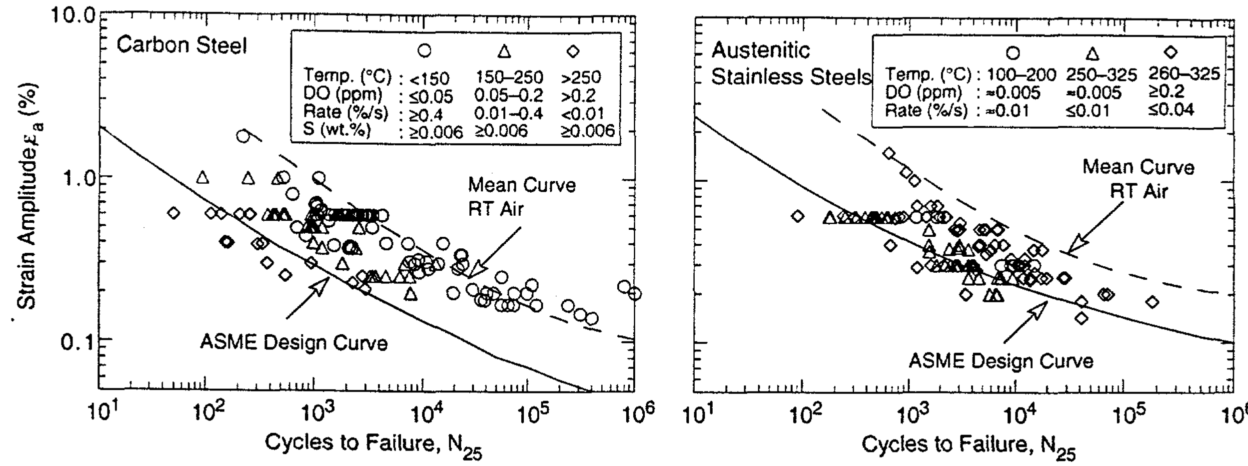

Figure 1. Fatigue S–N data for carbon steels and austenitic stainless steels in water

components. The statistical models for carbon and low–alloy steels have been updated with a larger fatigue S–N data base.[15]

However, the interim design curve and statistical model for austenitic SSs were based on limited data. For example, nearly all of the data in water were obtained at high temperatures (280–320°C) and high levels of dissolved oxygen (DO) (0.2–8 ppm). The data were inadequate to define the loading and environmental conditions that can decrease fatigue life of austenitic SSs. The threshold for strain amplitude above which environment can decrease fatigue life, and the value of strain rate below which environmental effects saturate, were based on the data for carbon and low–alloy steels. Fatigue life in LWR environments was assumed to be independent of temperature. Furthermore, although the proposed interim fatigue design curve[12] for austenitic SSs was based on data obtained in high–DO water, the curve was recommended for use at all oxygen levels until additional data became available, on the assumption that this was a conservative estimate of the likely effect of DO. Recent experimental results indicate that this is not the case.[9] Also, effects of LWR environments on the fatigue lives of cast SSs have not been addressed.

This paper summarizes available data on the effects of various material and loading variables such as steel type, DO level, strain range, and strain rate, on the fatigue lives of wrought and cast austenitic SSs. The data have been analyzed to identify key parameters that influence fatigue life and define the threshold and saturation values of these parameters. Statistical models that were developed earlier for estimating the fatigue lives of austenitic SSs in LWR environments have been updated with a larger data base. The significance of the effect of environment on the current Code design curve is evaluated.

OVERVIEW OF FATIGUE S–N DATA

The relevant S–N data for austenitic SSs are the JNUFAD* data base and the data compiled by Jaske and O'Donnell[16] for developing fatigue design criteria for pressure vessel alloys. Fatigue tests by Conway et al.[17] and Keller[18] on Types 304 and 316 SSs in air are also included in the data base. In addition, tests in water have been conducted on austenitic SSs

---

* Private communication from M. Higuchi, Ishikawajima–Harima Heavy Industries Co., Japan, to M. Prager of the Pressure Vessel Research Council, 1992. The old data base "FADAL" has been revised and renamed "JNUFAD."

by General Electric Co. (GE) in a test loop at the Dresden 1 reactor[19,20] and at ANL.[8,9] The data base for austenitic SSs is composed of ≈500 tests in air (240 tests on 26 heats of Type 304 SS, 170 tests on 15 heats of Type 316 SS, and 90 tests on 4 heats of Type 316 NG) and ≈300 tests in water (135 tests for 9 heats of Type 304, 55 tests on 3 heats of Type 316 SS, and 100 for 4 heats of Type 316 NG). Nearly 60% of the tests in air were conducted at room temperature, 20% at 250–325°C, and 20% at 350–450°C. Nearly 90% of the tests in water were conducted between 260–325°C; the remainder were at lower temperatures. The data in water on Type 316NG have been obtained primarily at high DO levels (≥ 0.2 ppm) and those on Type 316 SS at low-DO levels (≤0.005 ppm); half the tests on Type 304 SS are at low-DO and the remaining at high-DO levels.

Air Environment

The existing fatigue S–N data indicate that the fatigue lives of Types 304 and 316 SS are comparable and those of Type 316NG are superior. Fatigue life in air is independent of temperature in the range from room temperature to 427°C (Fig. 2). The three curves in Fig. 2 are based on the current ASME mean curve, the best-fit curve developed by Jaske & O'Donnell,[16] and an updated statistical model discussed later in the paper. The data for temperatures of 260–400°C indicate that the fatigue life of these steels decreases with decreasing strain rate (Fig. 3). Strain rate effects are not observed at room temperature. Above 260°C, the effect of strain rate on life seems to increase with increasing temperature.

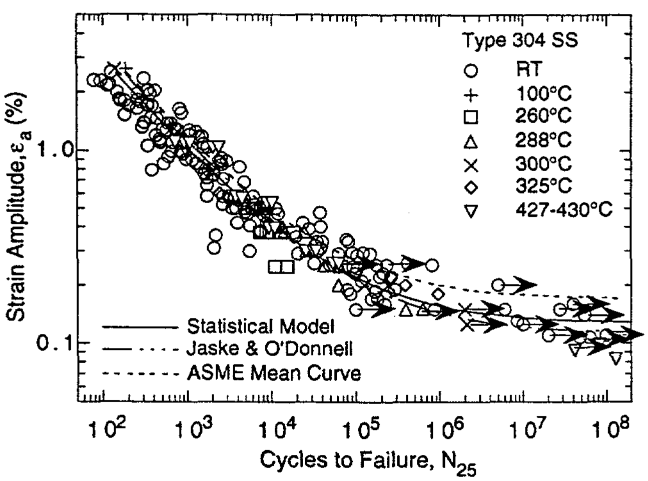

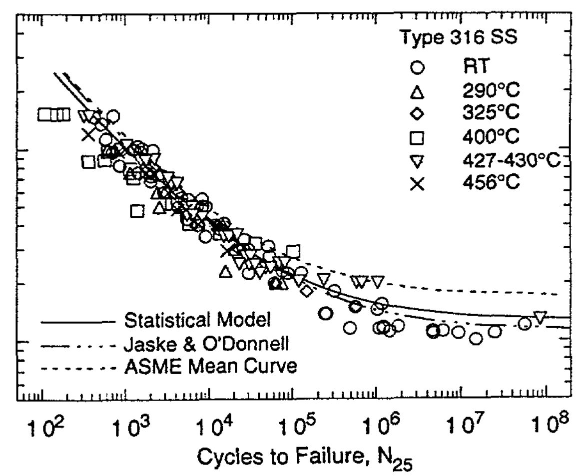

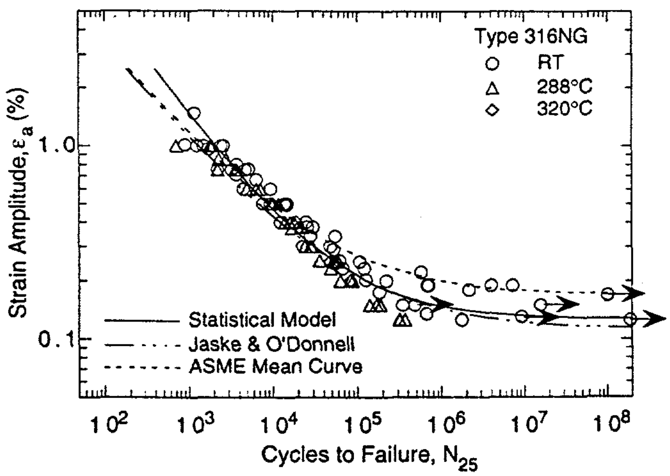

Fig. 2
Fatigue S–N behavior for Types 304, 316, and 316NG austenitic stainless steels in air at various temperatures

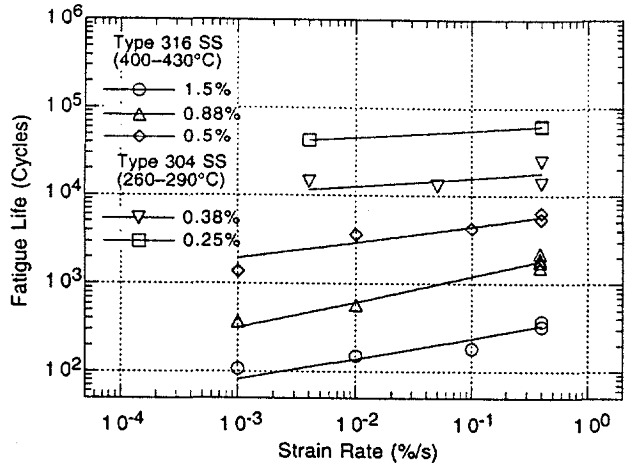

Fig. 3
Effect of strain rate on fatigue lives of austenitic SSs in air

During cyclic loading, austenitic SSs exhibit rapid hardening during the first 50–100 cycles. Extent of hardening increases with increasing strain amplitude and decreasing temperature and strain rate.[9] The initial hardening is followed by softening and a saturation stage at 288°C and by continuously softening at room temperature. For the various steels, cyclic stresses increase in the following order: Types 316NG, 304, and 316. The correlations for cyclic stress vs. strain curves are presented in Ref. 9.

LWR Environments

The fatigue S–N data indicate a significant decrease in fatigue life in LWR environments (Fig. 4). The reduction in life depends on strain rate, DO level in water, and temperature.[3–5,9] Also, environmental effects on fatigue life are comparable for all steels. A slow strain rate applied during the tensile-loading cycle is primarily responsible for environmentally assisted reduction in fatigue life. Slow rate applied during both tensile- and compressive-loading cycles does not cause further decrease in fatigue life.

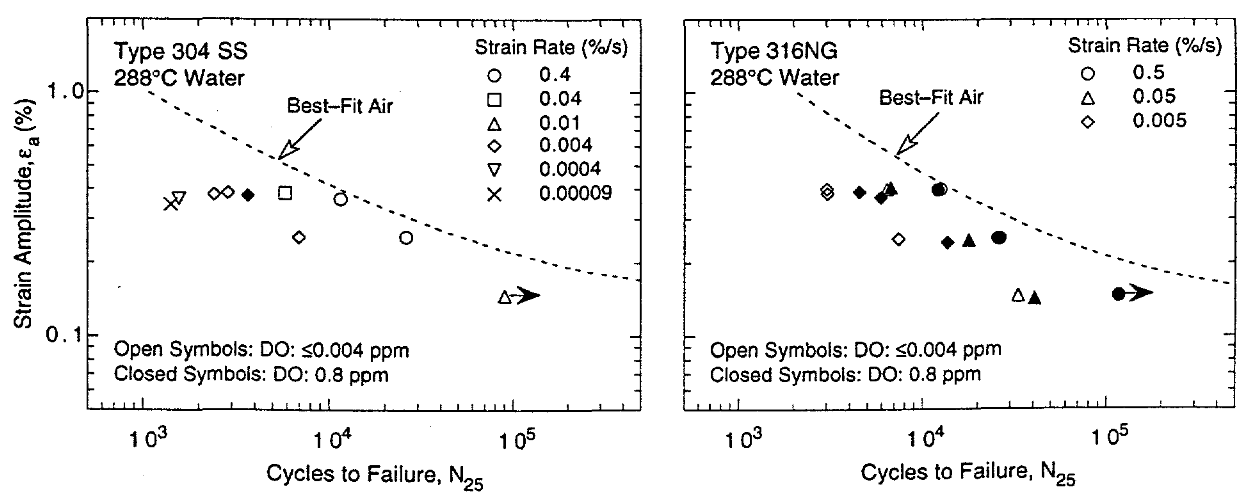

Figure 4. Fatigue S–N data for Types 304 and 316NG stainless steel in water at 288°C

The fatigue lives of austenitic SSs in low- and high-DO water are plotted as a function of tensile strain rate in Fig. 5. In both low- and high-DO levels, fatigue lives decrease with decreasing strain rate. The effect of strain rate is greater in a low-DO PWR environment than in high-DO water. In a simulated PWR environment, a decrease in strain rate from 0.4 to

0.004%/s decreases fatigue life by a factor of ≈8. The results indicate that the strain rate below which effects of strain rate on fatigue life saturate may depend both on steel type and DO level. In low–DO PWR environments, saturation strain rate appears to be at ≈0.0004%/s for Type 304 SS and ≈0.001%/s for Type 316 SS. The existing data are inadequate to establish saturation rate in high–DO water.

Results from exploratory tests,* where a slow strain rate is applied during only a fraction of the tensile loading cycle, indicate that a minimum threshold strain is required for environmentally assisted decrease in fatigue life of these steels. For a heat of Type 316 SS, the threshold strain in low–DO water at 325°C is ≈0.36% (Fig. 6). During each cycle, relative damage due to slow strain rate is the same once the strain amplitude exceeds the threshold value. Fatigue data from this study indicate a threshold strain range of ≈0.32% for the ANL heat of Type 304 SS (Fig. 4). The threshold strain most likely corresponds to rupture strain of the passive oxide film. These results are similar to those observed in carbon and low–alloy steels.[6,7]

The results also indicate that unlike carbon and low–alloy steels, environmental effects on the fatigue life of austenitic SSs are more pronounced in low–DO than in high–DO water.[3,9] At a strain rate of 0.004%/s, the reduction in fatigue life in a simulated PWR environment

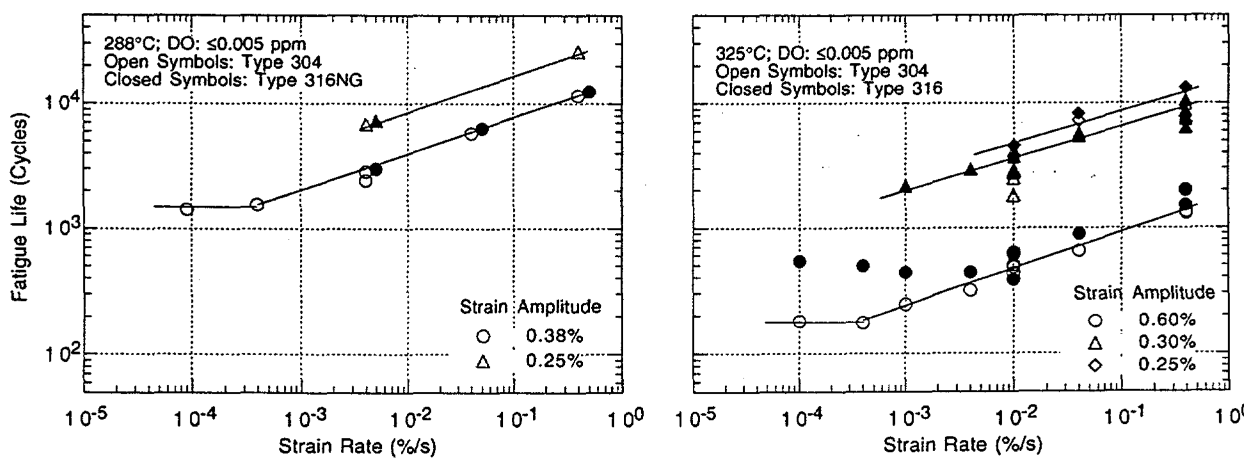

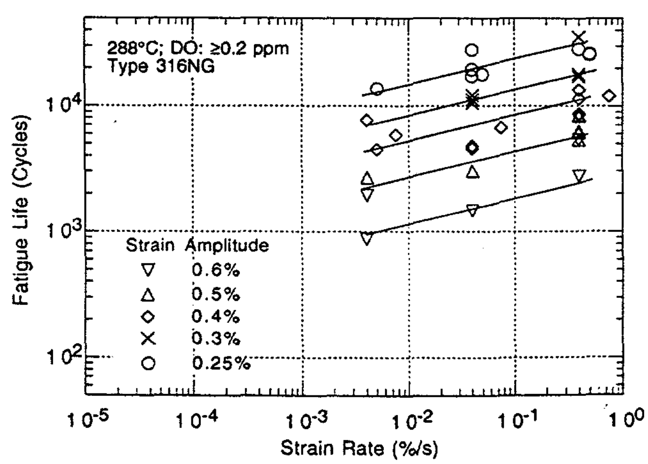

Figure 5
Dependence of fatigue life of austenitic stainless steels on strain rate in low– and high–DO water at various strain amplitudes

* H. Kanasaki, Mitshubishi Heavy Industries, Ltd., presented at the Pressure Vessel Research Council Meeting, February 1997, Las Vegas, NV.

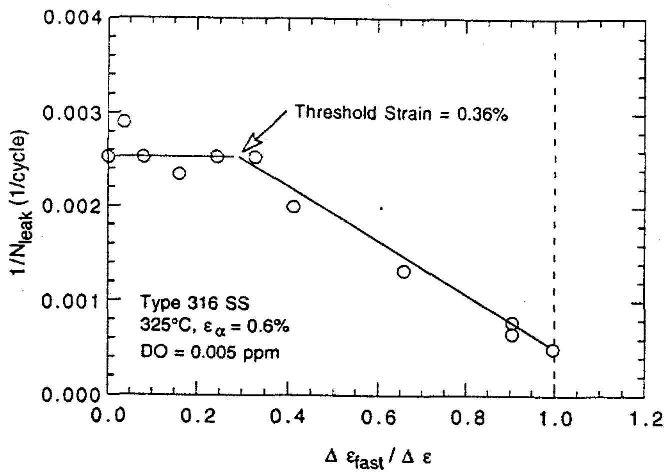

Fig. 6
Results of strain rate change tests on Type 316 SS in low-DO water at 325°C

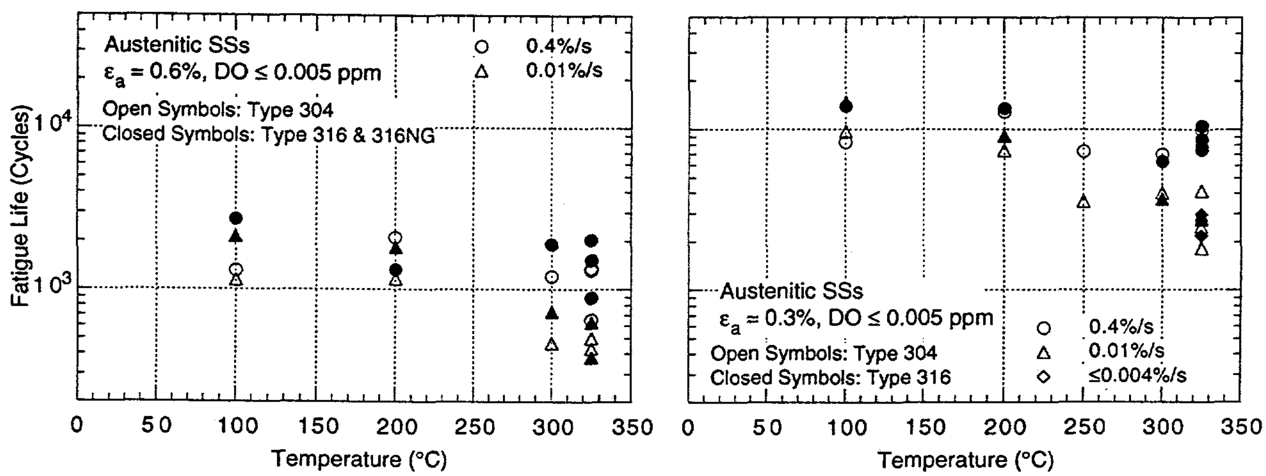

Figure 7. Change in fatigue life of austenitic stainless steels in low-DO water with temperature

(<0.01 ppm DO) is greater by a factor of ≈2 than in high-DO water (≥0.2 ppm DO). The existing data are inadequate to establish the functional form for the dependence of fatigue life of austenitic SSs on DO level. For carbon and low-alloy steels, environmental effects on fatigue life increase with increasing DO content above a minimum threshold value of 0.05 ppm; only a modest decrease in life is observed at DO levels < 0.05 ppm.[2,6,7,15]

The existing fatigue S–N data are inadequate to establish the dependence of life on temperature. Limited data indicate that environmental effects on fatigue life of austenitic SSs occur at temperatures above 250°C (Fig. 7). However, at 250–330°C, fatigue life appears to be relatively insensitive to changes in temperature. Only moderate decreases in life are observed at temperatures ≤ 200°C.

Cast Stainless Steels

The available fatigue S–N data indicate that in air, the fatigue life of cast CF-8 and CF-8M SSs is similar to that of wrought austenitic SSs. Thermal aging of cast SSs at temperatures between 300–400°C has no significant effect on fatigue properties, although the Charpy impact and fracture toughness properties are decreased significantly after thermal aging.[21] Results of fatigue crack growth studies indicate enhanced growth rates in PWR primary water, i.e., a factor of 2–10 increase in growth rate relative to that in air.[22,23] The enhancement is greater at high R–ratio and low values of ΔK than at low R–ratio and high ΔK values.[23]

The existing fatigue S–N data for cast SSs in LWR environments include the studies conducted at Mitsubishi Heavy Industries, Ltd. (MHI) in Japan* and the present work at ANL. The results indicate that the fatigue lives of cast SSs are approximately the same in both high– or low–DO water and are comparable to those observed for wrought SSs in low–DO water. Also, the reduction in life depends on strain rate (Fig. 9). The existing data are inadequate to establish the saturation strain rate for cast SSs. For unaged material, environmental effects on life do not appear to saturate at strain rates as low as 0.00001%/s. The results also indicate that the fatigue life of these steels is relatively insensitive to changes in ferrite content in the range of 12–28%.

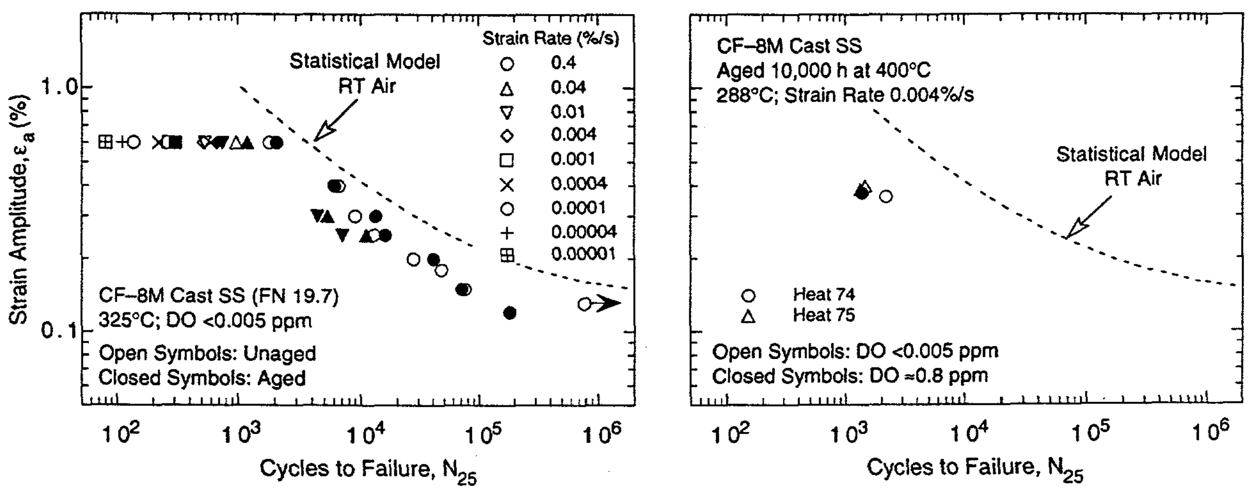

Figure 8. Fatigue S–N data for cast CF–8M stainless steel in water at 288 and 325°C

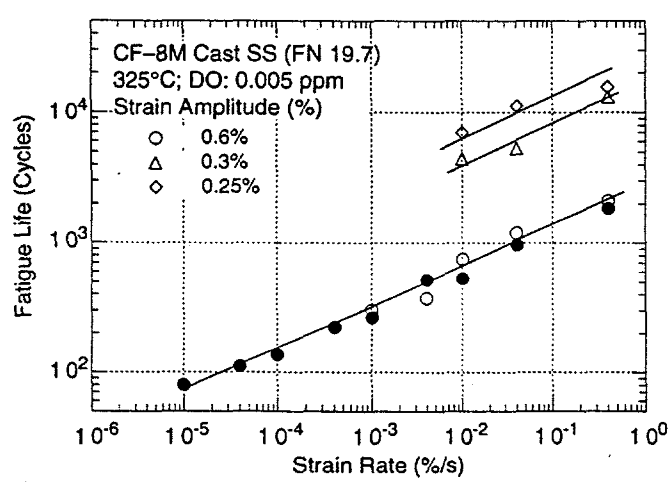

Fig. 9
Dependence of fatigue life of cast stainless steels on strain rate in low–DO water at various strain amplitudes

---

* H. Kanasaki, Mitshubishi Heavy Industries, Ltd., presented at the Pressure Vessel Research Council Meeting, October 1996, Columbus, OH.

MECHANISM OF FATIGUE CRACK INITIATION

The formation of surface cracks and their growth to an "engineering" size (3 mm deep) constitute the fatigue life of a material, which is represented by the fatigue S–N curves. Fatigue life has conventionally been divided into two stages: (a) initiation, expressed as the cycles to form microcracks on the surface; and (b) propagation, expressed as cycles to propagate the surface cracks to an engineering size. An alternative approach considers fatigue life to be entirely composed of the growth of short surface cracks.[24] In polycrystalline materials, the period for the formation of surface cracks is negligible; surface cracks, 10 μm or longer, form quite early in life.[7,25,26]

The enhanced growth rates of long cracks in pressure vessel and piping steels in LWR environments have been attributed to either slip oxidation/dissolution[27] or hydrogen-induced cracking[28] mechanisms. Both mechanism are dependent on the rates of oxide rupture, passivation, and liquid diffusion. Therefore, it is often difficult to differentiate between the two processes or to establish their relative contribution to crack growth in LWR environments. Studies on crack initiation in smooth fatigue specimens indicate that the decrease in fatigue life of carbon and low-alloy steels in LWR environments is caused primarily by the effects of environment on the growth of cracks < 100 μm deep.[7,14] Relative to air, crack growth rates in high-DO water are nearly two orders of magnitude higher for crack sizes < 100 μm and one order of magnitude higher for crack sizes > 100 μm. In LWR environments, crack initiation in carbon and low-alloy steels may be explained as follows: (a) surface microcracks form quite early in fatigue life; (b) during cyclic loading, the protective oxide film is ruptured at strains greater than the fracture strain of surface oxides, and the microcracks grow by anodic dissolution of the freshly exposed surface; and (c) growth of large cracks is characterized by accelerating growth rates.

For austenitic SSs, lower fatigue lives in low-DO water than in high-DO water are difficult to reconcile in terms of the slip oxidation/dissolution mechanism. In general, crack growth rates increase with increasing DO in water. It may be argued that the lower lives in low-DO water are due to a lower rupture strain for surface oxides in low-DO than in high-DO water. As discussed above, oxide rupture strain in low-DO water may be in the range of 0.32–0.36%. The rupture strain in high-DO water has to be significantly higher than this value to result in a factor of ≈2 difference in fatigue life.

Metallographic examination of the test specimens indicate that environmentally assisted reduction in fatigue life of austenitic SSs is most likely caused by hydrogen-induced cracking.[9] Figure 10 shows photomicrographs of the fracture surface, after chemical cleaning, at approximately the same crack length for Type 304 SS specimens tested in air, high-DO water, and low-DO simulated PWR environment. All specimens show fatigue striations; the spacing between striations indicate that crack growth increases in the following sequence: air, high-DO water, and low-DO PWR water. The presence of well defined striations suggests that the enhanced crack growth rates in austenitic SSs are most likely due to hydrogen-induced cracking. Fatigue striations should not be observed if enhancement of crack growth was caused by the slip dissolution/oxidation process.

STATISTICAL MODEL

The fatigue S–N curves are generally expressed in terms of the Langer equation, which may be used to represent either strain amplitude in terms of life or life in terms of strain

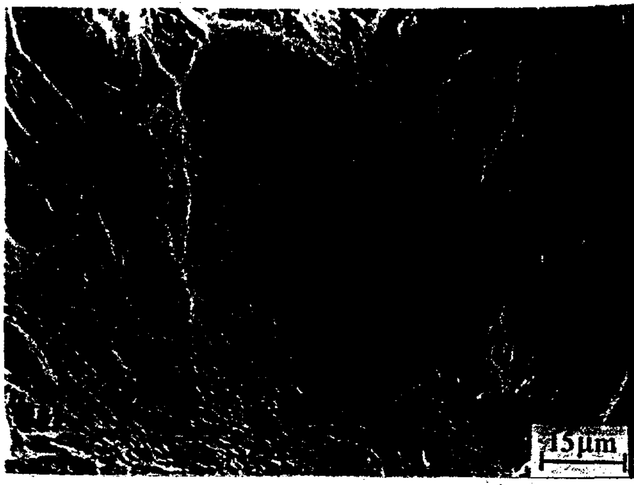

Air

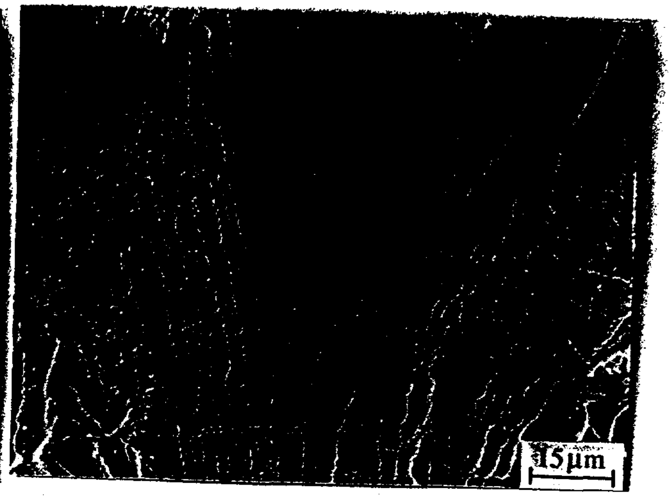

High–DO Water

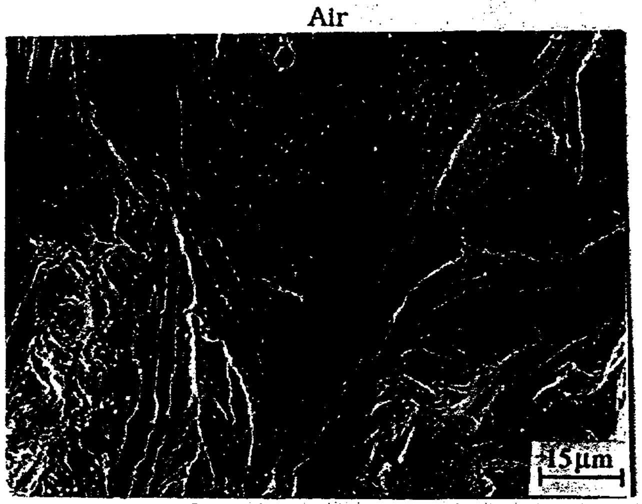

Simulate PWR Water

Figure 10
Photomicrographs of the fracture surface of Type 304 SS specimens tested at 288°C and 0.75% strain range in air, high–DO water, and low–DO simulated PWR water

amplitude. The parameters of the equation are commonly established through least–squares curve–fitting of the data to minimize the sum of the square of the residual errors for either strain amplitude or fatigue life. Statistical models have been developed by combining the two approaches and minimizing the sum of the squared Cartesian distances from the data point to the predicted curve.[13,14] The functional forms and transformation for the different variables were based on experimental observations and data trends. The models presented in Refs. 13 and 14 have been modified and updated with a larger fatigue S–N data base.

In air, the model assumes that fatigue life is independent of temperature and that strain rate effects occur at temperatures > 250°C. The effect of strain rate on life is considered to depend on temperature. In LWR environments, the fatigue life of austenitic SSs depends on strain rate, DO level, and temperature. The decrease in life is greater at low–DO levels and high temperatures. However, the existing data are inadequate to establish the functional form for the dependence of fatigue life on DO level or temperature. Separate correlations have been developed for low– and high–DO levels (< or ≥ 0.05 ppm), and low and high temperatures (< or ≥ 200°C). Also, a threshold strain rate of 1%/s and saturation rate of 0.0004%/s is assumed in the model. In air, the fatigue N of Types 304 and 316 SS is expressed as

$$\ln(N) = 6.703 - 2.030\ \ln(\varepsilon_a - 0.126) + T^{*}\ \dot{\varepsilon}^{*} \qquad (1a)$$

and that of Type 316NG as

$$\ln(N) = 7.422 - 1.671 \ln(\varepsilon_a - 0.126) + T^* \dot{\varepsilon}^*, \quad (1b)$$

where ε_a is the strain amplitude (%) and T^* and $\dot{\varepsilon}^*$ are transformed temperature and strain rate, respectively, defined as follows:

$$T^* = 0 \quad (T < 250°C)$$
$$T^* = [(T - 250)/525]^{0.84} \quad (250 \le T < 400°C) \quad (2a)$$

$$\dot{\varepsilon}^* = 0 \quad (\dot{\varepsilon} > 0.4\%/s)$$
$$\dot{\varepsilon}^* = \ln(\dot{\varepsilon}/0.4) \quad (0.0004 \le \dot{\varepsilon} \le 0.4\%/s)$$
$$\dot{\varepsilon}^* = \ln(0.0004/0.4) \quad (\dot{\varepsilon} < 0.0004\%/s). \quad (2b)$$

In LWR environments, the fatigue of Types 304 and 316 SS is expressed as

$$\ln(N) = 5.768 - 2.030 \ln(\varepsilon_a - 0.126) + T^* \dot{\varepsilon}^* O^* \quad (3a)$$

and that of Type 316NG as

$$\ln(N) = 6.913 - 1.671 \ln(\varepsilon_a - 0.126) + T^* \dot{\varepsilon}^* O^*, \quad (3b)$$

where the constants for transformed temperature, strain rate, and DO are defined as follows:

$$T^* = 0 \quad (T < 200°C)$$
$$T^* = 1 \quad (T \ge 200°C) \quad (4a)$$

$$\dot{\varepsilon}^* = 0 \quad (\dot{\varepsilon} > 0.4\%/s)$$
$$\dot{\varepsilon}^* = \ln(\dot{\varepsilon}/0.4) \quad (0.0004 \le \dot{\varepsilon} \le 0.4\%/s)$$
$$\dot{\varepsilon}^* = \ln(0.0004/0.4) \quad (\dot{\varepsilon} < 0.0004\%/s) \quad (4b)$$

$$O^* = 0.260 \quad (DO < 0.05\ ppm)$$
$$O^* = 0.172 \quad (DO \ge 0.05\ ppm). \quad (4c)$$

The model is recommended for predicted fatigue lives $\le 10^6$ cycles. One data set, obtained on Type 316 SS in room-temperature air, was excluded from the analysis. The tests were conducted in load-control mode at stress levels in the range of 190–230 MPa. The strain amplitudes were calculated only as elastic strains, i.e., strain amplitudes of 0.1–0.12% (the data are shown as circles in Fig. 2 with fatigue lives of 4×10^5 to 3×10^7). Based on cyclic stress vs. strain correlations for Type 316 SS,[9] actual strain amplitudes for these tests should be 0.23–0.32%. Furthermore, in LWR environments, the best-fit of the experimental data yielded a different slope for the S–N curve than that obtained in air; constants for the second term in Eqs. 3a and 3b were lower than those in air, particularly for Types 304 and 316 SS. For convenience in incorporating environmental effects into fatigue evaluations, the slope of the S–N curve in LWR environments was assumed to be the same as that in air.

The experimental values of fatigue life in air and water and those predicted from Eqs. 1–4 are plotted in Fig. 11. The estimated fatigue S–N curves for Types 304, 316, and 316NG SSs in air and LWR environments are shown in Figs. 2 and 12, respectively. The predicted fatigue lives show good agreement with the experimental data. Note that the ASME mean curve is not

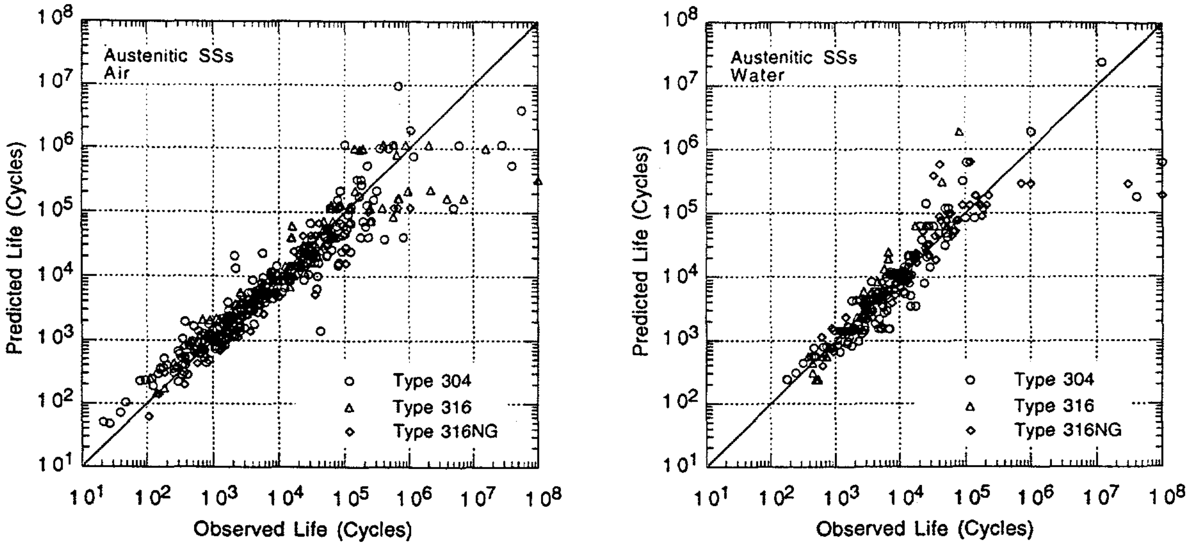

Figure 11. Experimental and predicted values of fatigue life of austenitic stainless steels in air and water environments

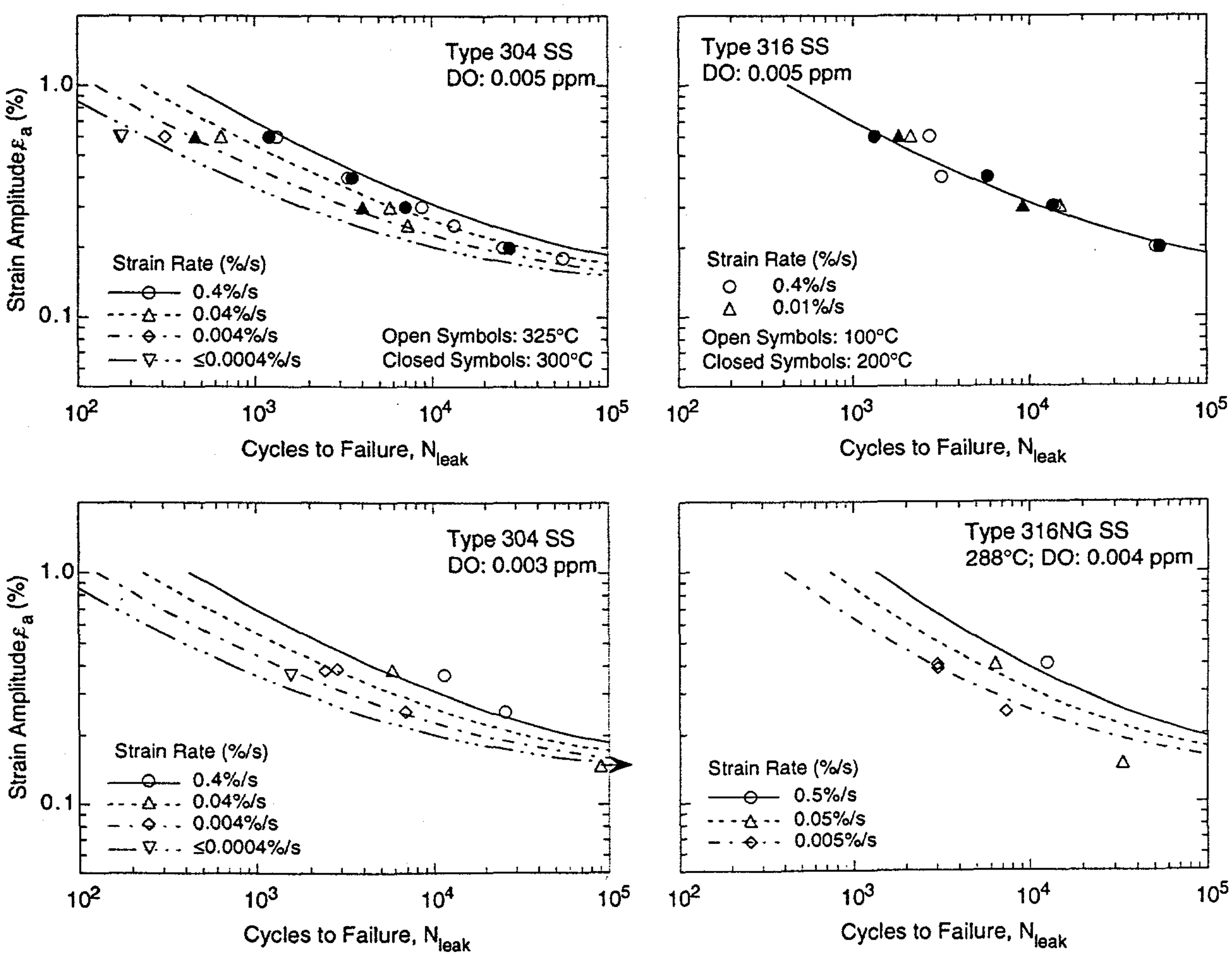

Figure 12. Experimental fatigue lives and S–N curves estimated from statistical models for austenitic stainless steels in water environments

consistent with the existing fatigue S–N data. In LWR environments, estimated values at low strain amplitudes are somewhat higher than the experimental values because, as discussed above, the slope of the S–N curve in water was assumed to be the same as in water, although best–fit of the data gave a steeper slope.

DESIGN FATIGUE CURVES

The current ASME Section III Code design fatigue curves were based on experimental data on small polished test specimens. The best–fit curve to the experimental data, expressed in terms of strain amplitude ε_a (%) and fatigue cycles N, for austenitic SSs is given by

$$\ln[N] = 6.954 - 2.0 \ln(\varepsilon_a - 0.167). \tag{5}$$

The mean curve, expressed in terms of stress amplitude S_a (MPa), which is the product of ε_a and elastic modulus E, is given by

$$S_a = 58020/\sqrt{N} + 299.92. \tag{6}$$

The room–temperature value of 195.1 GPa (28300 ksi) for the elastic modulus was used in converting the experimental strain–versus–life data to stress–versus–life curves. The best–fit curves were adjusted for the effect of mean stress by using the modified Goodman relation. The design fatigue curves were then obtained by lowering the adjusted best–fit curve by a factor of 2 on stress or 20 on cycles, whichever was more conservative, to account for differences and uncertainties in fatigue life associated with material and loading conditions.

The same procedure has been used to develop design fatigue curves for LWR environments. However, because of the differences between the ASME mean curve and the best–fit curve to existing fatigue data (Fig. 2), the margin on strain for the current ASME Code design fatigue curve is lower than 2. Therefore, a factor of 1.5 rather than 2 was used in developing the design fatigue curves from the statistical models in air and LWR environments.

The design fatigue curves based on the statistical model for Types 304 and 316 SS in air and low– and high–DO water are shown in Figs. 13–15. A similar set of curves can be obtained from Eqs. 1b and 3b for Type 316NG SS. Because the fatigue life of Type 316NG is superior to that of Types 304 or 316 SS, Figs. 13–15 may be used conservatively for Type 316NG SS. In air, although the differences at low stress levels between the current ASME Code design curve and the design curve obtained from the updated statistical model at temperatures < 250°C have been reduced or eliminated by reducing the margin on stress from 2 to 1.5, significant differences still exist between the two curves. For example, at stress amplitudes > 300 MPa, estimates of life from the updated design curve are a factor of ≈2 lower than those from the ASME Code curve. Also, because of strain rate effects at temperatures > 250°C, estimated fatigue lives may be further reduced up to a factor of ≈3.5 at very slow strain rates.

As discussed above, the existing fatigue data indicate a threshold strain range of ≈0.32%, below which environmental effects on fatigue life of austenitic SSs either do not occur or are insignificant. This value must be adjusted for the effects of mean stress and uncertainties due to material and loading variability. Threshold strain amplitudes are decreased by ≈10% to account for mean stress effects and by a factor of 1.5 to account for uncertainties in fatigue life associated with material and loading variability. Thus, a threshold strain amplitude of 0.097%

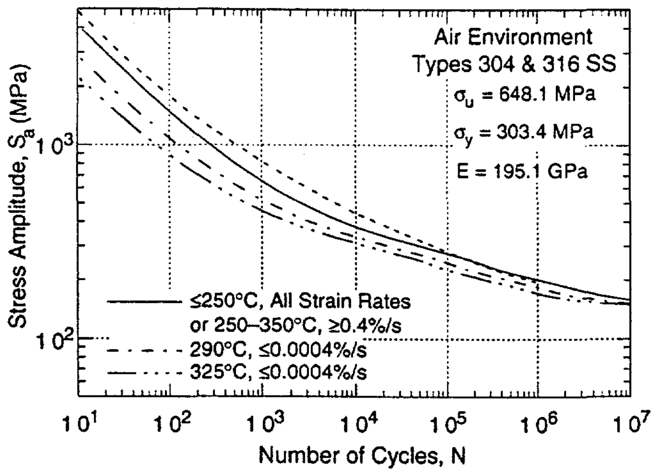

Fig. 13
Design fatigue curves for Types 304 and 316 stainless steel in air

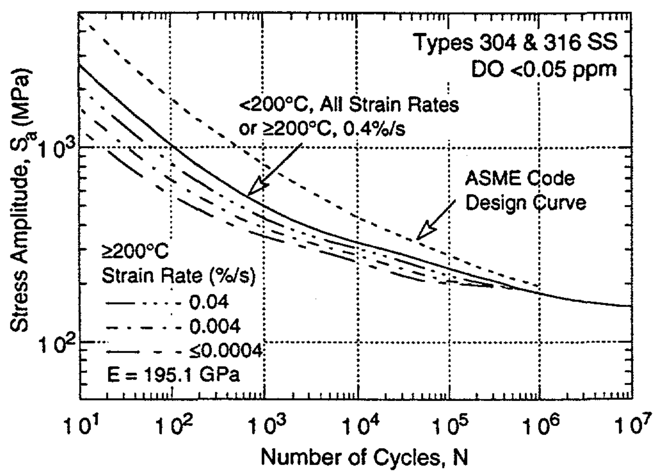

Fig. 14
Design fatigue curves for Types 304 and 316 stainless steel in water with <0.05 ppm dissolved oxygen

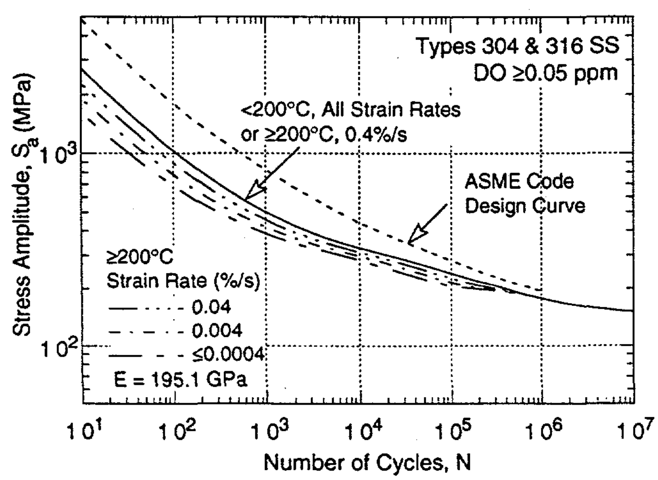

Fig. 15
Design fatigue curves for Types 304 and 316 stainless steel in water with ≥0.05 ppm dissolved oxygen

(stress amplitude of 189 MPa) was selected, below which environmental effects on life are modest and are represented by the design curve for temperatures < 200°C (shown by the solid line in Figs. 14 and 15). Note that the design curves in LWR environments not only account for environmental effects on life but also include the difference between the current Code design curve and the updated design curve in air, i.e., the difference between the solid and dashed curves in Fig. 13.

FATIGUE LIFE CORRECTION FACTOR

The effects of reactor coolant environments on fatigue life have also been expressed in terms of a fatigue life correction factor F_{en}, which is the ratio of the life in air at room temperature to that in water at the service temperature.[2,29] To incorporate environmental effects into the ASME Code fatigue evaluation, a fatigue usage for a specific load pair based on the current Code fatigue design curve is multiplied by the correction factor. A fatigue life correction factor F_{en} can also be obtained from the statistical model, where

$$\ln(F_{en}) = \ln(N_{air}) - \ln(N_{water}). \tag{7}$$

From Eqs. 1a and 2a, the fatigue life correction factor relative to room–temperature air for Types 304 and 316 SSs is given by

$$F_{en} = \exp(0.935 - T^* \dot{\varepsilon}^* O^*), \tag{8}$$

where the threshold and saturation values for T^*, $\dot{\varepsilon}^*$ and O^* are defined in Eqs. 4a–4c. At temperatures ≥ 200°C and strain rates ≤ 0.0004%/s, Eq. 8 yields an F_{en} of ≈15 in low–DO PWR water (< 0.05 ppm DO) and ≈8 in high–DO water (≥ 0.05 ppm DO). At temperatures < 200°C, F_{en} is ≈2.5 in both low– and high–DO water at all strain rates.

SUMMARY

The existing fatigue S–N data for austenitic stainless steels in air and water environments have been evaluated to establish the effects on the fatigue life of these steels due to various material and loading variables such as steel type, strain range, strain rate, temperature, and DO level in water. In air, the fatigue lives of austenitic SSs are independent of temperature in the range from room temperature to 450°C. At temperatures ≥250°C, fatigue life decreases with decreasing strain rate. Also, the fatigue lives of Types 304 and 316 SS are comparable and those of Type 316NG are superior. For all steels, cyclic stresses increase with decreasing strain rate and are 20–30% lower at 288–430°C than at room temperature. The results indicate that the current ASME mean curve is not consistent with the existing fatigue S–N data.

The results in LWR environments indicate a significant decrease in fatigue life in water relative to that in air; the decrease in life depends on strain rate, DO level in water, and temperature. Environmental effects on fatigue life are comparable for all steels. However, unlike those in carbon and low–alloy steels, environmental effects are more pronounced in low–DO than in high–DO water. The influence of reactor environments on fatigue crack initiation is discussed.

Statistical models for estimating the fatigue S–N curves as a function of material, loading, and environmental variables have been updated with a larger fatigue data base. Design fatigue curves have been developed for austenitic SS components in LWR environments. The effects of LWR coolant environments on fatigue life have also been expressed in terms of a fatigue life correction factor defined as the ratio of the life in air to that in water.

ACKNOWLEDGMENTS

The authors thank W. F. Burke, T. M. Galvin, and J. Tezack for their contributions to the experimental effort. This work was sponsored by the Office of Nuclear Regulatory Research, U.S. Nuclear Regulatory Commission, FIN Number W6610; Program Manager: Dr. M. McNeil.

REFERENCES

1. ASME Boiler and Pressure Vessel Code Section III – Rules for Construction of Nuclear Power Plant Components, The American Society of Mechanical Engineers, New York, 1994 Ed.

2. Higuchi, M., and Iida, K., "Fatigue Strength Correction Factors for Carbon and Low–Alloy Steels in Oxygen–Containing High–Temperature Water," *Nucl. Eng. Des.* **129**, pp. 293–306, 1991.

3. Higuchi, M., and Iida, K., "Reduction in Low–Cycle Fatigue Life of Austenitic Stainless Steels in High–Temperature Water," in *Pressure Vessel and Piping Codes and Standards*, PVP Vol. 353, D. P. Jones, B. R. Newton, W. J. O'Donnell, R. Vecchio, G. A. Antaki, D. Bhavani, N. G. Cofie, and G. L. Hollinger, eds., American Society of Mechanical Engineers, New York, pp. 79–85, 1997.

4. Mimaki, H., Kanasaki, H., Suzuki, I., Koyama, M., Akiyama, M., Okubo, T., and Mishima, Y., "Material Aging Research Program for PWR Plants," in *Aging Management Through Maintenance Management*, PVP Vol. 332, I. T. Kisisel, ed., American Society of Mechanical Engineers, New York, pp. 97–105, 1996.

5. Fujiwara, M., Endo, T., and Kanasaki, H., "Strain Rate Effects on the Low Cycle Fatigue Strength of 304 Stainless Steel in High Temperature Water Environment," in *Fatigue Life: Analysis and Prediction, Proc. of the Intl. Conf. and Exposition on Fatigue, Corrosion Cracking, Fracture Mechanics, and Failure Analysis*, ASM, Metals Park, OH, pp. 309–313, 1986.

6. Chopra, O. K., and Shack, W. J., "Evaluation of Effects of LWR Coolant Environments on Fatigue Life of Carbon and Low–Alloy Steels," in *Effects of the Environment on the Initiation of Crack Growth*, ASTM STP 1298, W. A. Van Der Sluys, R. S. Piascik, and R. Zawierucha, eds., American Society for Testing and Materials, Philadelphia, pp. 247–266, 1997.

7. Chopra, O. K., and Shack, W. J., "Effects of LWR Coolant Environments on Fatigue Design Curves of Carbon and Low–Alloy Steels,' NUREG/CR–6583, ANL–97/18, Feb. 1998.

8. Shack, W. J., and Burke, W. F., "Fatigue of Type 316NG SS," in *Environmentally Assisted Cracking in Light Water Reactors, Semiannual Report, October 1989–March 1990*, NUREG/CR–4667 Vol. 10, ANL–91/5, pp. 3–19, March 1991.

9. Chopra, O. K., and Gavenda, D. J., "Effects of LWR Coolant Environments on Fatigue Lives of Austenitic Stainless Steels," in *Pressure Vessel and Piping Codes and Standards*, PVP Vol. 353, D. P. Jones, B. R. Newton, W. J. O'Donnell, R. Vecchio, G. A. Antaki, D. Bhavani, N. G. Cofie, and G. L. Hollinger, eds., American Society of Mechanical Engineers, New York, pp. 87–97, 1997.

10. Van Der Sluys, W. A., "Evaluation of the Available Data on the Effect of the Environment on the Low Cycle Fatigue Properties in Light Water Reactor Environments," in *Proc. 6th Intl. Symp. on Environmental Degradation of Materials in Nuclear Power Systems – Water Reactors*, R. E. Gold and E. P. Simonen, eds., The Metallurgical Society, Warrendale, PA, pp. 1–4, 1993.

11. Van Der Sluys, W. A., and Yukawa, S., "Status of PVRC Evaluation of LWR Coolant Environmental Effects on the S–N Fatigue Properties of Pressure Boundary Materials," in *Fatigue and Crack Growth: Environmental Effects, Modeling Studies, and Design Considerations*, PVP Vol. 306, S. Yukawa, ed., American Society of Mechanical Engineers, New York, pp. 47–58, 1995.

12. Majumdar, S., Chopra, O. K., and Shack, W. J., "Interim Fatigue Design Curves for Carbon, Low–Alloy, and Austenitic Stainless Steels in LWR Environments," NUREG/CR-5999, ANL-93/3, April 1993.

13. Keisler, J., Chopra, O. K., and Shack, W. J., "Fatigue Strain–Life Behavior of Carbon and Low–Alloy Steels, Austenitic Stainless Steels, and Alloy 600 in LWR Environments," NUREG/CR-6335, ANL-95/15, Aug. 1995.

14. Keisler, J., Chopra, O. K., and Shack, W. J., "Fatigue Strain–Life Behavior of Carbon and Low–Alloy Steels, Austenitic Stainless Steels, and Alloy 600 in LWR Environments," *Nucl. Eng. Des.* **167**, pp. 129–154, 1996.

15. Chopra, O. K., and Shack, W. J., "Fatigue Crack Initiation in Carbon and Low–Alloy Steels in Light Water Reactor Environments: Mechanisms and Prediction," these proceedings.

16. Jaske, C. E., and O'Donnell, W. J., *Fatigue Design Criteria for Pressure Vessel Alloys*, Trans. ASME J. Pressure Vessel Technology **99**, 584–592, 1977.

17. Conway, J. B., Stentz, R. H., and Berling, J. T., *Fatigue, Tensile, and Relaxation Behavior of Stainless Steels*, TID–26135, U.S. Atomic Energy Commission, Washington, DC, 1975.

18. Keller, D. L., *Progress on LMFBR Cladding, Structural, and Component Materials Studies During July, 1971 through June, 1972, Final Report, Task 32*, Battelle–Columbus Laboratories, BMI–1928, 1977.

19. Hale, D. A., Wilson, S. A., Kiss, E., and Gianuzzi, A. J., *Low Cycle Fatigue Evaluation of Primary Piping Materials in a BWR Environment*, GEAP–20244, U.S. Nuclear Regulatory Commission, Sept. 1977.

20. Hale, D. A., Wilson, S. A., Kass, J. N., and Kiss, E., *Low Cycle Fatigue Behavior of Commercial Piping Materials in a BWR Environment*, J. Eng. Mater. Technol. **103**, 15–25, 1981.

21. Slama, G., Petrequin, P., and Mager, T., "Effect of Aging on Mechanical Properties of Austenitic Stainless Steel Castings and Welds," in *Assuring Structural Integrity of Steel Reactor Pressure Boundary Components*, SMiRT Post Conference Seminar 6, Monterey, CA (1983).

22. Amzallag, C., Baudry, G., and Bernard, J. L., "Effects of PWR Environment on the Fatigue Crack Growth of Different Stainless Steels and Inconel Type Alloy," in *Proc. Int. Atomic Energy Agency Specialists' Meeting on Subcritical Crack Growth, Vol. 1*, NUREG/CP-0044, U.S. Nuclear Regulatory Commission, pp. 163–194, 1983.

23. Hanninen, H., Torronen, K., Kemppainen, M., and Cullen, B., "Environment-Sensitive Cyclic Crack Growth of CF8M Cast Stainless Steel in PWR Primary Water," in ???.

24. Miller, K. J., "Damage in Fatigue: A New Outlook," in *International Pressure Vessels and Piping Codes and Standards: Volume 1 – Current Applications*, PVP Vol. 313-1, K. R. Rao and Y. Asada, eds., American Society of Mechanical Engineers, New York, pp. 191–192, 1995.

25. Gavenda, D. J., Luebbers, P. R., and Chopra, O. K., "Crack Initiation and Crack Growth Behavior of Carbon and Low-Alloy Steels," in *Fatigue and Fracture 1*, Vol. 350, S. Rahman, K. K. Yoon, S. Bhandari, R. Warke, and J. M. Bloom, eds., American Society of Mechanical Engineers, New York, pp. 243–255, 1997.

26. Tokaji, K., Ogawa, T., and Osaka, S., "The Growth of Microstructurally Small Fatigue Cracks in a Ferrite-Pearlite Steel," *Fatigue Fract. Engng. Mater. Struct.* **11**, pp. 311–342, 1988.

27. Ford, F. P., "Overview of Collaborative Research into the Mechanisms of Environmentally Controlled Cracking in the Low Alloy Pressure Vessel Steel/Water System," in *Proc. 2nd Int. Atomic Energy Agency Specialists' Meeting on Subcritical Crack Growth*, NUREG/CP-0067, MEA-2090, Vol. 2, pp. 3–71, April 1986.

28. Hänninen, H., Törrönen, K., and Cullen, W. H., "Comparison of Proposed Cyclic Crack Growth Mechanisms of Low Alloy Steels in LWR Environments," in *Proc. 2nd Int. Atomic Energy Agency Specialists' Meeting on Subcritical Crack Growth*, NUREG/CP-0067, MEA-2090, Vol. 2, pp. 73–97, April 1986.

29. Mehta, H. S., and Gosselin, S. R., "An Environmental Factor Approach to Account for Reactor Water Effects in Light Water Reactor Pressure Vessel and Piping Fatigue Evaluations," in *Fatigue and Fracture Volume 1*, PVP Vol. 323, H. S. Mehta, ed., American Society of Mechanical Engineers, New York, pp. 171–185, 1996.